Human Fructosamine-3-Kinase

Purification, Sequencing, Substrate Specificity, and Evidence of Activity In Vivo

Benjamin S. Szwergold, Scott Howell, and Paul J. Beisswenger

Nonenzymatic glycation appears to be an important factor in the pathogenesis of diabetic complications. Key early intermediates in this process are fructosamines, such as protein-bound fructoselysines. In this report, we describe the purification and characterization of a mammalian fructosamine-3-kinase (FN3K), which phosphorylates fructoselysine (FL) residues on glycated proteins, to FL-3-phosphate (FL3P). This phosphorylation destablilizes the FL adduct and leads to its spontaneous decomposition, thereby reversing the nonenzymatic glycation process at an early stage. FN3K was purified to homogeneity from human erythrocytes and sequenced by means of electrospray tandem mass spectrometry. The protein thus identified is a 35-kDa monomer that appears to be expressed in all mammalian tissues. It has no significant homology to other known proteins and appears to be encoded by genomic sequences located on human chromosomes 1 and 17. The lability of FL3P, the high affinity of FN3K for FL, and the wide distribution of FN3K suggest that the function of this enzyme is deglycation of nonenzymatically glycated proteins. Because the condensation of glucose and lysine residues is an ubiquitous and unavoidable process in homeothermic organisms, a deglycation system mediated by FN3K may be an important factor in protecting cells from the deleterious effects of nonenzymatic glycation. Our sequence data of FN3K are in excellent agreement with a recent report on this enzyme by Delpierre et al. (*Diabetes* 49:1627–1634, 2000). *Diabetes* 50: 2139–2147, 2001

From the Department of Medicine, Dartmouth Medical School, Hanover, New Hampshire.

Address correspondence and reprint requests to Benjamin S. Szwergold, PhD, Department of Medicine, Dartmouth Medical School, HB 7515, Vail 601, Hanover, NH 03755. E-mail: szwergold@dartmouth.edu.

Received for publication 26 October 2000 and accepted in revised form 25 May 2001.

3DF, 3-deoxyfructose; 3DG, 3-deoxyglucosone; AGE, advanced glycation end product; BLAST, Basic Local Alignment Search Tool; CDTA, cyclohexyldiamine-tetraacetic acid; C3, carbon 3; DAN, diaminonaphthalene; DGA, 3-deoxy-2-ketogluconic acid; EST, expressed sequence tag; FBAPZ, fructose-1,4-(3-aminoethyl)-piperazine; FDAB-8, fructose-(polypropyleninimine octaamine dendrimer); FL, fructoselysine; FL3P, FL-3-phosphate; FN3K, fructosamine-3-kinase; Fru-3P, fructose-3-phosphate; GCMS, gas chromatography–mass spectrometry; HPLC, high-performance liquid chromatography; IEF, isoelectric focusing; ManL-3P, mannitol-lysine-3-phosphate; MDPA, methylene-diphosphonic acid; μLC/MS/MS, microcapillary reverse-phase HPLC nano-electrospray tandem mass spectrometry; MS/MS, tandem mass spectrometry; NCBI, National Center for Biotechnology Information; NMR, nuclear magnetic resonance; ORF, open reading frame; PCR, polymerase chain reaction; PPA, phenyl phosphonic acid; SorL-3P, sorbitol-lysine-3-phosphate; TMS, trimethylsilyl.

Nonenzymatic glycation (Maillard reaction) is a process in which glucose and other sugars react spontaneously with amine-containing molecules, such as proteins (1,2). These reactions proceed through many stages, starting with glucosylamines (Schiff bases), fructosamines (Amadori compounds) (3,4), and aminoaldoses (Heyns compounds) (5,6) and ultimately lead to the formation of irreversible end products, which include crosslinks, aromatic heterocycles (2,7,8), and oxidized compounds (9,10), that are designated collectively as advanced glycation end products (AGEs) (11). The concentrations of these products are elevated in diabetes, and evidence from numerous studies suggest that nonenzymatic glycation and AGE formation may be important in the etiology of diabetes complications (12–14).

In our previous studies of the cataract in the diabetic rat lens, we identified fructose-3-phosphate (Fru-3P), which is a novel, potent glycating agent (15, 16). Our data suggested that this compound is produced through the phosphorylation of fructose by a fructose-3-phosphokinase (18), the activity of which was detected in other tissues, such as rat and human sciatic nerves, bovine vagal nerves, the bovine retina, pancreas, and kidneys, the rat heart, and human erythrocytes (19).

During further investigation, we discovered that this enzyme phosphorylates a wide variety of fructosamines with affinities orders-of-magnitude greater than its affinity for fructose. An especially interesting aspect of the substrate specificity of fructosamine-3-kinase (FN3K) is that it readily phosphorylates fructoselysine (FL) residues on glycated proteins, resulting in the production of protein-bound FL-3-phosphate (FL3P) (17). Because of the proximity of the keto group and the phosphate in FL3P, this phosphoester is labile and decomposes readily by β-elimination to regenerate an unmodified lysine residue, with inorganic phosphate and 3-deoxyglucosone (3DG) as byproducts.

Because of the apparent involvement of FN3K in the process of nonenzymatic glycation, we purified this enzyme to homogeneity using human erythrocytes as a convenient source. The enzyme (a 35-kDa monomeric protein) was characterized functionally and sequenced by means of electrospray tandem mass spectrometry (MS/MS). The sequence thus obtained was used to identify a number of expressed sequence tags (ESTs), from which a

complete open reading frame (ORF) nucleotide sequence of FN3K was deduced. The data thus obtained are in excellent agreement with the FN3K sequence recently published by Delpierre et al. (20).

The high affinity of the FN3K for FL on proteins and the lability of FL3P suggest that this kinase may be part of an ATP-dependent system for removing carbohydrates from nonenzymatically glycated proteins. This hypothesis is supported by analysis of Hb from normoglycemic individuals and diabetic patients, which shows that phosphorylation of protein-bound FL residues occurs in vivo and that extreme hyperglycemia leads to an accumulation of Hb-bound FL3P. Finally, based on the information available, it appears that production of Fru-3P in the lens and other tissues is merely a corollary side effect of the essential function of FN3K as a deglycating enzyme.

RESEARCH DESIGN AND METHODS

Materials. Common reagents were purchased from Sigma and Aldrich. Lysine-rich histones were obtained from Sigma (Type III-S, H 5505), and 6-thio-D-fructose was purchased from ICN Pharmaceuticals. ^{33}P-ATP was purchased from NEN. Image ESTs were obtained from Incyte Genomics and Research Genetics. High-quality human cDNA and polymerase chain reaction (PCR) reagents were purchased from Clonetech.

Synthetic procedures. Fru-3P was synthesized as previously described (15). FL was synthesized by an adaptation of the method of Finot and Mauron (21). Other Amadori compounds were synthesized by refluxing a mixture of 250 mmol/l base, 250 mmol/l glucose, 50 mmol/l sodium-metabisulfite, and 1.25 mol/l acetic acid in 100 ml of H_2O/MeOH solution for 4 h. The Amadori products were purified on a Dow-50 cation exchange column as described by Roper et al. (4). Concentrations of the Amadori products were determined by ^{13}C nuclear magnetic resonance (NMR) spectroscopy on a Bruker AM-400 spectrometer at 100.6 MHz, using 45° pulses and 6-s relaxation delay without NOE decoupling and with signal averaging of 400–10,000 scans.

Affinity resin. CNBr-activated Sepharose (10 ml) was hydrated in 100 ml of 1 mmol/l HCl. The hydrated resin was packed onto a 20 × 2.5 cm column and washed with 200 ml of 1 mmol/l HCl. After this wash, the resin was incubated for 1 h with a 50-ml solution of 100 mmol/l fructose-(polypropyleninimine octaamine dendrimer) (FDAB-8) in coupling buffer (100 mmol/l $NaHCO_3$ and 500 mmol/l NaCl, pH 8.3). After completion of the coupling reaction, excess reagents were removed and extensively washed with coupling buffer. Finally, the column was equilibrated with buffer A (10 mmol/l Tris, 1.0 mmol/l dithiothreitol, and 0.1 mmol/l phenylthanolamine fluoride; pH 7.5) and stored at 4°C.

Purification of FN3K. Two units of outdated erythrocytes from a blood bank were washed with three volumes of wash buffer (10 mmol/l phosphate and 0.9% NaCl, pH 7.5), and the erythrocytes were pelleted by centrifugation for 20 min at 3,000*g*. After removal of the supernatant and buffy coat, the pellet was washed four times with 3–4 volumes of wash buffer. After the final wash, cells were lysed hypotonically by adding four volumes of buffer A and stirring for 5 min at 4°C. The lysate was loaded onto a 1,000-ml DEAE cellulose column and washed with buffer A supplemented with 10 mmol/l KCl to remove the bulk of the Hb. Washing was continued until the eluate became colorless. The enzyme was eluted with 1.25 l of buffer A supplemented with 400 mmol/l KCl. The preparation was subsequently fractionated with $(NH_4)_2SO_4$, with the peak FN3K activity found between 40 and 60% $(NH_4)_2SO_4$. The ammonium sulfate pellet was dialyzed overnight against 2 l of buffer A and loaded onto a smaller DEAE cellulose column (215 × 50 mm diameter). The sample was eluted with a 1.2 l gradient of 10–400 mmol/l KCl in buffer A, with a single peak at 150 mmol/l KCl. Pooled fractions were concentrated to 5 ml by ultrafiltration in Centriprep centrifugal concentrators (Millipore) and passed through a Toyopearl–50 gel filtration column (100 × 2.5 cm diameter). FN3K activity eluted as a single peak at a position equivalent to a protein with a molecular weight of 34–35 kDa.

Pooled peak fractions from the gel filtration column were concentrated to 0.5 ml by centrifugal ultrafiltration using Ultrafree-4 centrifugal concentrators (Millipore) and stored at −40°C. Unless otherwise indicated, all of our experiments on substrate specificity and kinetic properties of FN3K were performed using this preparation.

Final purification of the enzyme to homogeneity was achieved by a combination of affinity chromatography using an FDAB-8-Sepharose column and isoelectric focusing (IEF). Peak fractions from the gel filtration column were diluted to 4 ml and loaded onto a 5-ml FBAD-8-Sepharose column. The resin was washed with 10 ml of buffer A, followed by 10 ml of buffer A containing 100 mmol/l KCl. FN3K was eluted with 20 ml of 2.5 mmol/l FDAB (pH 7.5). Peak FN3K fractions from the affinity column were concentrated to ~50 μl in Ultrafree 0.5 centrifugal concentrators and fractionated further by IEF on a vertical minigel (BioRad) at 4°C. After electrophoresis, the IEF gel was cut into 1-mm slices. One-quarter of each slice was homogenized and assayed for FN3K activity, and the remaining portion of the gel was stored in individual Eppendorf tubes for further processing. After completion of the FN3K assay on the IEF fractions, protein was removed by electroelution from the gel slices with the highest FN3K activity and analyzed on SDS-PAGE. Purified FN3K showed peak activities on the IEF gel at pH 6.8 and 7.1 and migrated as a single 35-kDa band on SDS-PAGE.

FN3K assay. Enzyme preparations of 75-μl aliquots were added to an assay mixture containing 50 mmol/l HEPES (pH 8.0), 5 mmol/l ATP, 0.5 μCi of ^{33}P-ATP, 2 mmol/l $MgCl_2$, and 1 mmol/l of FBAPZ (fructose-1,4-[3-aminoethyl]-piperazine), with a final volume of 100 μl. The assay mixture was incubated at 37°C for 60 min, and the reaction was stopped with an equal volume (100 μl) of 25 mmol/l EDTA. Aliquots of the incubation mixture (95 μl) were spotted in duplicate on 2.5-cm diameter phosphocellulose paper disks (Whatman P-81). The disks were air dried then washed extensively with deionized water. The washed filters were placed in 7-ml scintillation vials with 5 ml of scintillation fluid and counted. In each assay, three controls were included: *1*) a positive control using partially purified FN3K, *2*) negative controls using incubation mixtures without substrate, and *3*) negative controls using the standard incubation mixture, supplemented with 10 mmol/l cyclohexyl-diamine-tetraacetic acid (CDTA) to inhibit the FN3K reaction.

Amadori phosphoesters. Phosphorylation of the Amadori products was performed by incubating aliquots of the enzyme preparation with 5 mmol/l of substrate, 50 mmol/l ATP, and 12.5 mmol/l $MgCl_2$ in 200 mmol/l HEPES (pH 8.0) for 12 h (total volume 1 ml). At the conclusion of the incubation, the reaction was stopped by adding 200 μl of 250 mmol/l CDTA. ^{31}P NMR spectra of the kinase products were collected at 162 MHz on a Bruker-AM 400 NMR spectrometer using 60° pulses, with signal averaging of 2,000–50,000 free induction decays. ^{31}P NMR chemical shifts were referenced to glycerophosphorylcholine at 0.49 ppm.

Glycated proteins. Glycated histones were made by incubating 100 mg of lysine-rich histones at 37°C for 4 weeks with 1 mol/l glucose in 100 mmol/l HEPES buffer (pH 7.5) containing 0.1% sodium azide. At the end of the incubation, the protein was dialyzed against deionized water, concentrated to 50 mg/ml, and analyzed by ^{13}C NMR spectroscopy for presence of FL, which was found at a concentration of 148 μmol/g protein. Similar protocols were used to glycate other proteins, such as lysozyme and bovine serum albumin.

Decomposition of FL3P. To assess the stability of FL3P, preparations of this compound were incubated in a neutral buffer (50 mmol/l HEPES, pH 7.5) at 37°C in an NMR sample tube in the NMR spectrometer. ^{31}P NMR spectra were collected at hourly intervals, and aliquots of the incubation solution were taken at intervals of 2–3 h to assay for 3DG.

3DG assays. These assays were performed using a gas chromatography–mass spectrometry (GCMS) assay system developed in our laboratory and previously described in detail (22). Briefly, 3DG was reacted with 2,3 diaminonaphthalene (DAN), extracted by ethyl acetate, and derivatized to its trimethylsilyl (TMS) derivative. The derivatized sample was analyzed on a Shimadzu QP-5000 GC MS system equipped with a QP-5050 mass selective detector and AOC-20i automatic sampler using a method described previously. The major fragments generated by the DAN-TMS adduct of 3DG were at a charge/mass ratio (m/z) of 295 and 306. Concentrations of 3DG were determined by comparing the two fragments from unlabeled 3DG with those from a [U-^{13}C]-labeled 3DG standard generating ions at an m/z of 299 and 309.

FL3P on Hb. Hb was obtained from samples of frozen erythrocytes (4–12 ml) of three normoglycemic volunteers and seven diabetic patients. The frozen pellets were thawed in four volumes of water and reduced by dialyzing them overnight against 500 ml of water containing 1 g $NaBH_4$. At the conclusion of the reduction, the preparations were dialyzed for another 12 h against 4.0 l of 50 mmol/l phosphate buffer (pH 7.5) and two changes of deionized water. After dialysis, samples were reconcentrated back to their starting volumes using Centriprep centrifugal concentrators. During the final step of the concentration process, HEPES buffer (pH 8.0) and CDTA were added to a final concentration of 100 and 25 mmol/l, respectively. The final concentration of Hb in the sample was determined by a specific colorimetric assay (23). The amounts of FL3P were determined by comparing the integrated peak intensities of the two reduction products of FL3P (sorbitol-lysine-3-phosphate and mannitol-lysine-3-phosphate) in ^{31}P NMR spectra with peak intensities of two internal concentration standards, methylene-diphosphonic acid (MDPA) and phenyl phosphonic acid (PPA).

Substrate	Net charge	Apparent K_m (μmol/l)	Relative apparent V_{max} (%)
Fructose	0	50,000	35
6-deoxy-6-thiofructose	0	25,000	35
Fructoseglycine	0	6,500	35
Fructosevaline	0	6,000	100
1-deoxy-1-morpholino-fructose	+1	500	100
FL	+1	750	100
Fructoseornithine	+1	500	100
Fructose-1,3-diaminopropane	+2	150	100
Fructosespermidine	+3	15	100
FBAPZ	+3	25	50
Fructosespermine	+4	5	100

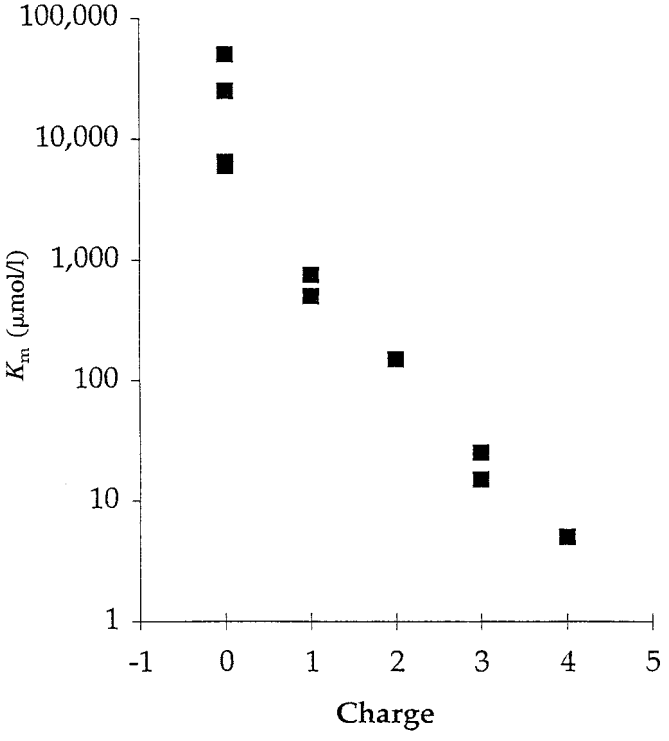

FIG. 1. Affinity of FN3K for fructose and fructose adducts as a function of the net positive charge of the substrate. The apparent K_ms of eleven substrates are plotted.

HbA_{1c}. Measurements of HbA_{1c} were performed using the Diamat high-performance liquid chromatography (HPLC) system (24).

Protein analysis and sequencing. Protein bands from the SDS-PAGE gels containing ~10 μg were cut out and placed in plain Eppendorf tubes. The gel slices were rinsed for 1 min with water/methanol (1:1) then washed twice for 2 min with 50% acetonitrile. After removal of excess fluid, the samples were frozen and shipped on dry ice for analysis. Sequence analysis was performed at the Harvard Microchem Facility by microcapillary reverse-phase HPLC nano-electrospray tandem mass spectrometry (μLC/MS/MS) on a Finnigan LCQ quadrupole ion trap mass spectrometer.

PCR analysis. Based on the deduced ORF sequence for FN3K, five PCR primers were synthesized at the Dartmouth Molecular Biology Core Facility. These primers included one reverse primer at position 867 of the ORF and four forward primers at positions 103, 213, 480, and 680 of the ORF. Screening for FN3K expression in tissues was performed using a 209-bp amplimer between positions 680 and 889 of the ORF.

PCR reactions were performed on a GeneApm PCR system-2400 (Perkin-Elmer) using an AdvantageTaq PCR kit from Clonetech.

DNA sequence analysis and alignment. Homology searches for ESTs were performed using the Basic Local Alignment Search Tool (BLAST) at the (National Center for Biotechnology Information (NCBI) web site, and sequence alignments of the DNA sequences were performed using DNA-star software at Dartmouth's Center for Biological and Biomedical Computing.

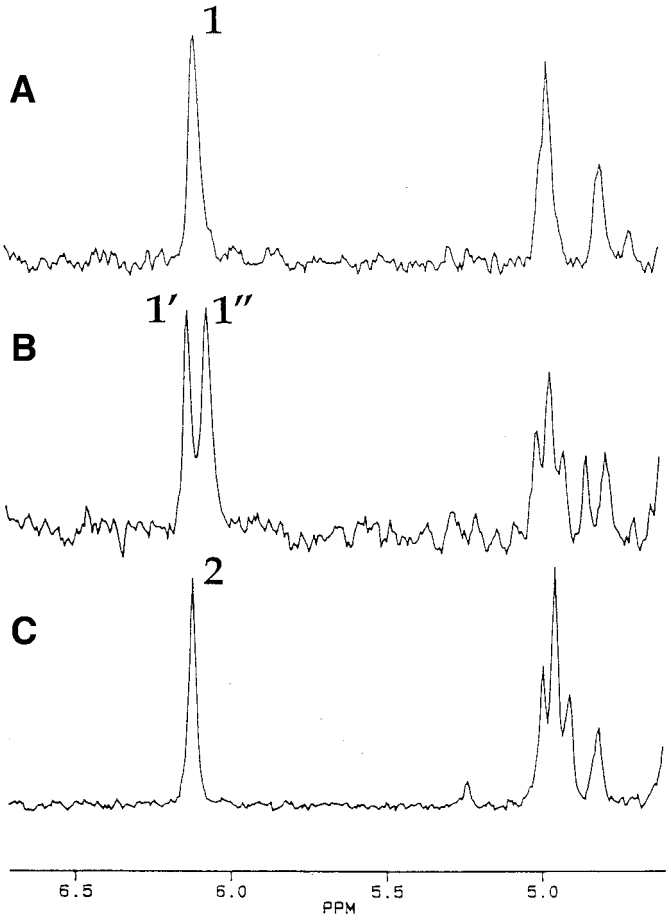

FIG. 2. *A*: Proton-decoupled ^{31}P NMR spectrum of FBAPZ-3-phosphate (peak 1). *B*: Proton-coupled ^{31}P NMR spectrum of FBAPZ-3-phosphate. Because of the spin-spin coupling between the ^{31}P nucleus of the phosphate and the proton on the adjacent carbon, the phosphorus resonance on this compound is split into a doublet with a ^{31}P-^{1}H coupling constant of 10.5 (peaks 1′ and 1″). *C*: Proton-coupled ^{31}P NMR spectrum of [3′-^{2}H]FBAPZ-3-phosphate (peak 2). Replacement of the C3 proton with a deuteron eliminates the spin-spin coupling effect seen in *B*. This site-specific effect of deuterium demonstrates conclusively that the phosphoester is located at the C3 position of fructose.

RESULTS

Substrate specificity. To characterize the phosphokinase that phosphorylates fructose to Fru-3P (18,19), we used outdated human erythrocytes as a convenient source of this enzyme. During the process of purification of this protein, we discovered that, in addition to fructose, this kinase also catalyzes the ATP-dependent phosphorylation of fructosamines (1-amino-1-deoxy fructose derivatives, such as FL and fructose-spermine). Products of this reaction are novel phosphoesters that appear as unique peaks between 5.8 and 6.3 ppm in the ^{31}P NMR spectra, making them easily differentiable from other phosphomonoesters whose ^{31}P chemical shifts are generally clustered between 1.0 and 5.2 ppm (25).

The kinase is specific for 1-deoxy-1-amino fructose adducts and does not catalyze phosphorylation of other monosaccharides and polyols, such as glucose, galactose, mannose, glucosamine, galactosamine, or *myo*-inositol. As detailed in Fig. 1, this enzyme can tolerate a large variety

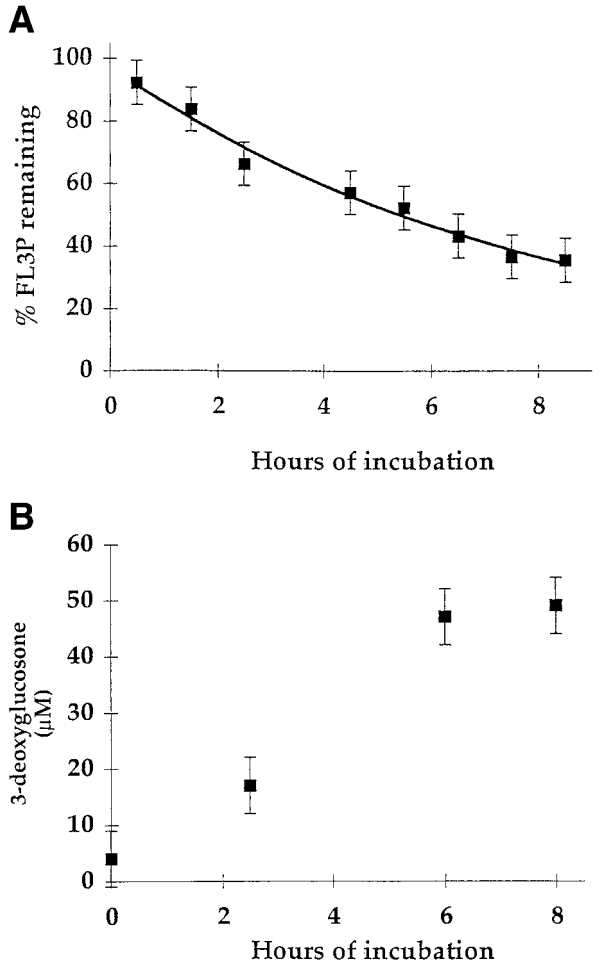

FIG. 3. *A*: Decomposition of FL3P incubated at 37°C in 50 mmol/l HEPES buffer (pH 7.5). *B*: Production of 3DG concurrent with the decomposition of FL3P during the incubation.

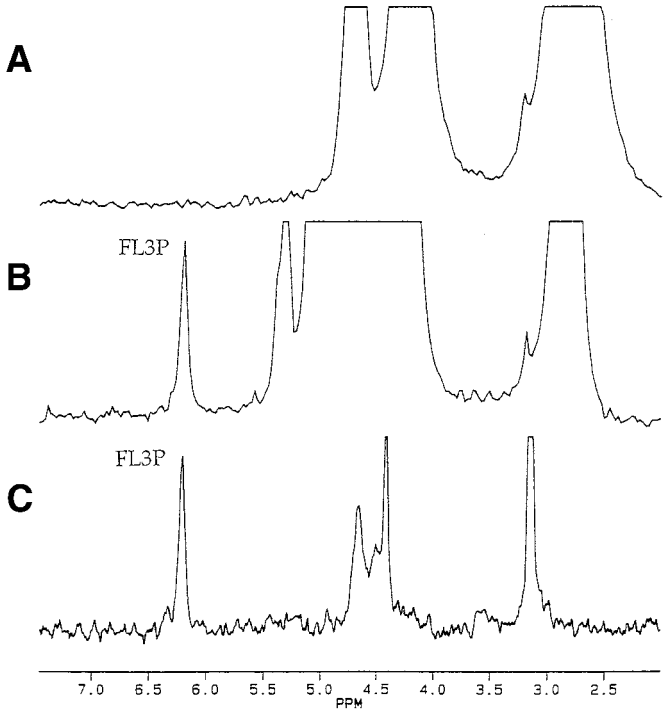

FIG. 4. *A*: Proton-decoupled ^{31}P NMR spectrum of native lysine-rich histones after a 12-h incubation with Mg-ATP and FN3K. *B*: Proton-decoupled ^{31}P NMR spectrum of glycated histones after a 12-h incubation with Mg-ATP and FN3K. *C*: Same sample as in *B* after a 12-h dialysis against deionized water.

of fructose-like substrates with bulky groups at the 1-N position and has a high affinity for N-substituents with net positive charge.

To determine the location of the phosphate ester on the fructose moiety, we compared ^{1}H-coupled ^{31}P NMR spectra of unlabeled fructosamine-phosphates with similar spectra of identical phosphofructosamine-phosphates labeled with deuterium at the carbon 3 (C3) of fructose. The results of these experiments, which are illustrated in Fig. 2, indicate that in these fructosamine-phosphates, the phosphoester is located on the C3 of the fructose moiety.

Stability of fructosamine-3-phosphates. Because our prior data from studies of Fru-3-P suggests that the proximity of the phosphate group to the carbonyl should make fructosamine-3-phosphate susceptible to -elimination (15,16), we examined the stability of several of these compounds. As anticipated, we found that fructosamine-3-phosphates are significantly more labile than Fru-3P, with a half-life of 5–6 h. An example of one such experiment is illustrated in Fig. 3, which shows the exponentially decreasing concentration of FL3P and a concurrent increase in 3DG during an incubation of a solution of 75 μmol/l FL3P at 37°C in a 50 mmol/l HEPES medium (pH 7.5).

Glycated proteins as substrates. Because the fructosamine most frequently encountered in nature is FL on glycated proteins (2,26), we examined the possibility that FN3K can phosphorylate these adducts. A preparation of glycated lysine-rich histones was incubated with Mg-ATP and a semipurified preparation of the kinase. As illustrated in Fig. 4*B*, an FL3P peak was readily visible in the ^{31}P NMR spectrum of this mixture after 12 h of incubation. To confirm that this peak was indeed caused by FL3P on protein, the reaction mixture was dialyzed extensively and then re-examined by ^{31}P NMR. After dialysis, the FL3P peak remained with the protein fraction, whereas the other small metabolites were dialyzed away (Fig. 4*C*), proving that the FL3P is associated with the protein. In subsequent experiments, we determined that the apparent K_m of the FN3K for histone-bound FL residues is ~10 μmol/l, which is ~75-fold lower than that of free FL (750 μmol/l) and ~5,000-fold lower than the K_m for fructose (50 mmol/l). Similar experiments with other glycated proteins, including Hb, bovine serum albumin, and lysozyme indicate that FL residues on glycated proteins are readily phosphorylated by FN3K, apparently irrespective of the protein.

Evidence of FN3K activity in vivo. The high affinity of FN3K for FL and for glycated proteins suggested that protein-bound FL may be the relevant substrate for this enzyme in vivo; consequently, one should be able to detect FL3P in glycated proteins of diabetic patients. To test this hypothesis, Hb from a poorly controlled patient (19% HbA_{1c}) was reduced with $NaBH_4$ to stabilize any putative FL3P and was examined by ^{31}P NMR.

As illustrated in Fig. 5*A*, $NaBH_4$ reduction of FL3P produces two polyol derivatives: SorL-3P and ManL-3P. ^{31}P NMR examination of the reduced Hb (Fig. 5*B*) showed two peaks at the approximate chemical shift positions of

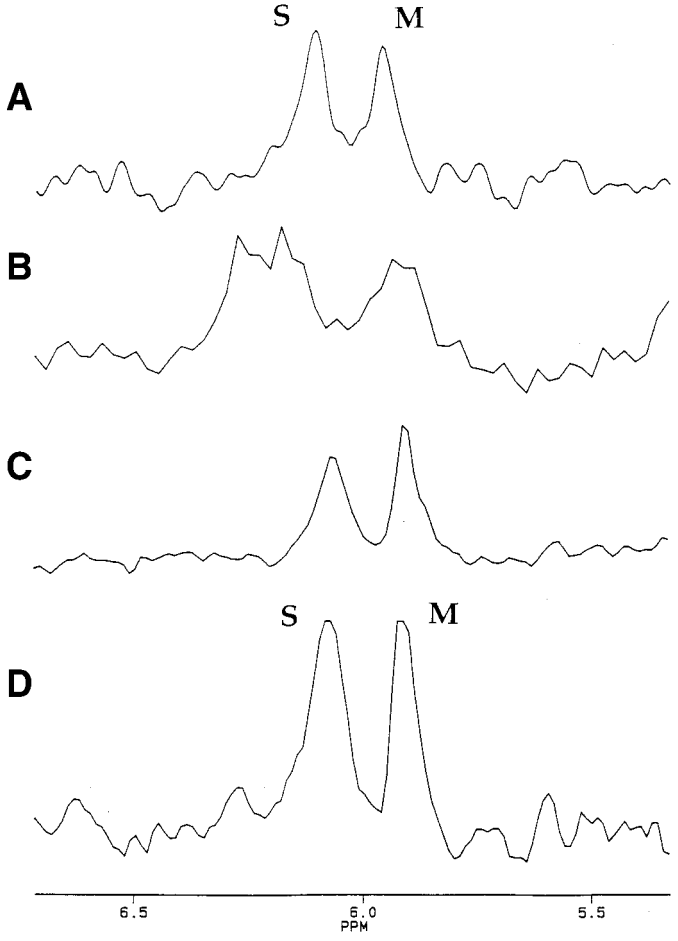

FIG. 5. Proton-decoupled ^{31}P NMR spectra. *A*: Phosphorylated and glycated histones after reduction with $NaBH_4$. *B*: 250 mg/ml Hb from a diabetic patient after reduction with $NaBH_4$. *C*: Same sample as in *B* after an overnight digestion with proteinase K. *D*: Same sample as in *C* after a spike with authentic SorL-3P (S) and ManL-3P (M).

SorL-3P and ManL-3P. However, because of the effects of the protein microenvironment (27), these two peaks were broad, and their chemical shifts did not coincide with those of free SorL-3P and ManL-3P. To minimize these effects and improve spectral resolution, the sample was digested overnight with proteinase K. As seen in Fig. 5*C*, this digestion greatly improved the quality of the NMR spectrum, especially by collapsing the previously broad and heterogeneous peak of SorL-3P into a relatively narrow resonance. The subsequent addition of authentic SorL-3P/ManL-3P derived from a digest of $NaBH_4$-reduced phosphorylated-glycated histone (Fig. 5*D*) showed that Hb-bound FL3P is indeed produced in vivo.

To examine the relationship between Hb-bound FL3P and long-term glycemia as indicated by HbA_{1c} (28,29), we measured the FL3P content of 10 Hb samples containing various amounts of HbA_{1c}. As can be seen in Fig. 6, this analysis showed that FL3P increases with increasing HbA_{1c}. However, this correlation is not linear; little or no FL3P was detected at HbA_{1c} values <8%, whereas FL3P content increases rapidly at HbA_{1c} values ≥8%.

Purification and characterization of FN3K. FN3K was purified to homogeneity (Fig. 7*B*) using a combination of ion exchange chromatography, size fractionation, affinity chromatography, and IEF (Table 1). Because of the instability of the purified enzyme, purification of this protein proved difficult, and the final yield of the purified protein was quite low. The purified enzyme was stabilized by prompt concentration to small volumes and by inclusion of 1 mol/l FBAPZ and 50% glycerol in frozen enzyme aliquots.

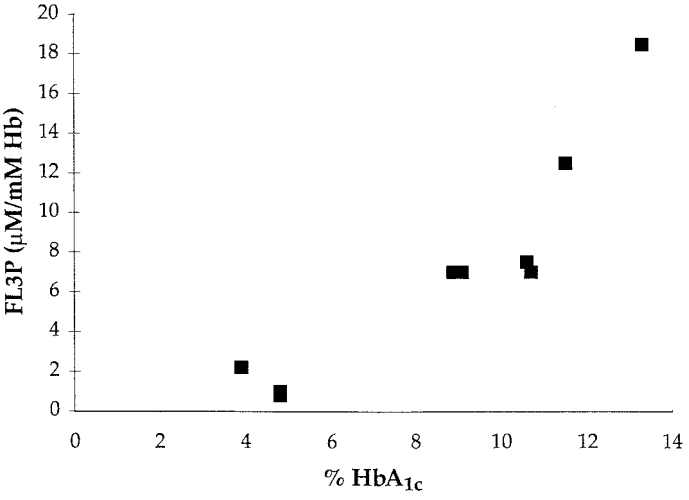

FIG. 6. Correlation between the percentage of HbA_{1c} and FL3P in Hb of 10 individuals (3 normoglycemic and 7 diabetic subjects) with varying degrees of glycemic control.

The purified protein was analyzed by μLC/MS/MS. This analysis resulted in the detection of 12 unique peptides that matched two mouse and two human ESTs in the NCBI

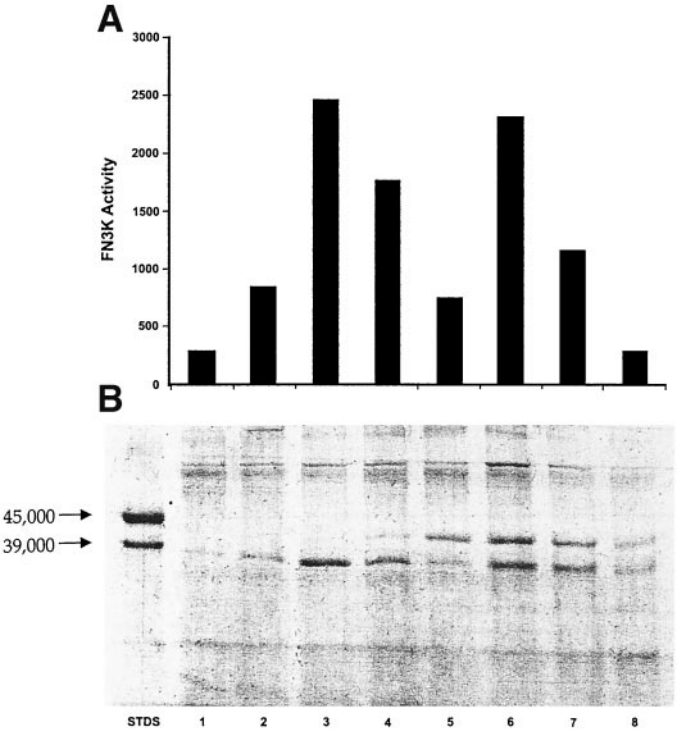

FIG. 7. *A*: Enzymatic activity of FN3K fractions from an IEF gel. *B*: SDS-PAGE of the IEF fractions assayed above. The two proteins in *lane 1* are 45 and 39 kDa molecular weight markers. The IEF gel slices range from pH 7.3 in slice 1 to pH 6.6 in slice 8, with peak FN3K activities occurring in slices 3 and 6. The higher molecular weight bands (39 kDa) in slices 6 and 7 were identified as hydroxymethylbilane synthase by μLC/MS/MS.

TABLE 1
Purification of FN3K

Step	Total protein (mg)	Total activity* (units)	Specific activity†	Purification	Yield (%)
Crude lysate	160,000	522	0.0033	1	—
DEAE-1	4,000	612	0.15	45.5	100
Ammonium sulfate ppt.	1,000	130	0.13	39.4	25
DEAE-2	288	42	146	44	8
Gel filtration (Toyopearl-50)	9	18	2	603	3.4
Affinity chromatography	1.6	14	8.8	2,660	2.7
IEF	0.032	4	125	38,000	0.6

*A unit of FN3K activity is defined as the micromoles per hour of FL phosphorylated to FL3P; †specific activity is defined as units of FN3k per milligram protein.

database. Based on homologies between these 4 ESTs and other ESTs in the database, we identified another 9 overlapping human ESTs and 28 overlapping mouse sequences. Alignment of these sequences produced a full-length ORF of 927 bp, with high-quality start and stop codons. This ORF sequence was refined using only data from human ESTs and translated to an amino acid sequence, resulting in a predicted protein sequence of 309 amino acids (Fig. 8) with a molecular weight of 35 kDa.

```
1     CGTCAAGCTTGGCACGAGGCC
22    ATGGAGCAGCTGCTGCGCGCCGAGCTGCGCACCGCGACCCTGCGGGCCTTC
1      M  E  Q  L  L  R  A  E  L  R  T  A  T  L  R  A  F
73    GGCGGCCCCGGCGCCGGCTGCATCAGCAAGGGCCGAGCCTACGACACGGAC
18     G  G  P  G  A  G  C  I  S  K  G  R  A  Y  D  T  D
124   GCAGGCCCAGTGTTCGTCAAAGTCAACCGCACGACGCATGCCCGGCCGATG
35     A  G  P  V  F  V  K  V  N  R  T  T  H  A  R  P  M
175   TTAGAGGGGGAGGTGGCCAGCCTGGAGGCCCTCCGGAGCACGGGCCTGGTG
52     L  E  G  E  V  A  S  L  E  A  L  R  S  T  G  L  V
226   CGGGTGCCGAGGCCCATGAAGGTCATCGACCTGCCGGGAGGTGGGGCCGCC
69     R  V  P  R  P  M  K  V  I  D  L  P  G  G  G  A  A
277   TTTGTGATGGAGCATTTGAAGATGAAGAGCTTGAGCAGTCAAGCATCAAAA
86     F  V  M  E  H  L  K  M  K  S  L  S  S  Q  A  S  K
328   CTTGGAGAGCAGATGGCAGATTTGCATCTTTACAACCAGAAGCTCAGGGAG
103    L  G  E  Q  M  A  D  L  H  L  Y  N  Q  K  L  R  E
379   AAGTTGAAGGAGGAGGAGAACACAGTGGGCCGAAGAGGTGAGGGTGCTGAG
120    K  L  K  E  E  E  N  T  V  G  R  R  G  E  G  A  E
430   CCTCAGTATGTGGACAAGTTCGGCTTCCACACGGTGACGTGCTGCGGCTGC
137    P  Q  Y  V  D  K  F  G  F  H  T  V  T  C  C  G  C
481   ATGCCGCAGGTGAATGAGTGGCAGGATGACTGGCCGACCTTTGTCACCCGG
154    M  P  Q  V  N  E  W  Q  D  D  W  P  T  F  V  T  R
532   CACCGGCTCCAGGCGCATCTGGACCTCATTGAGAAAGACTATGCTGACCGA
171    H  R  L  Q  A  H  L  D  L  I  E  K  D  Y  A  D  R
583   GAAGCACAAGAACTCTGGTCCCGGCTACAGGTGAAGATCCCGGATCTGTTT
188    E  A  Q  E  L  W  S  R  L  Q  V  K  I  P  D  L  F
634   TGTGGCCTAGAGATTGTCCCCGCGTTGCTCCACGGGGATCTCTGGTCGGGA
205    C  G  L  E  I  V  P  A  L  L  H  G  D  L  W  S  G
685   AACGTGGCTGAGGACGACGTGGGGCCCATTATTTACGACCCGGCTTCCTTC
222    N  V  A  E  D  D  V  G  P  I  I  Y  D  P  A  S  F
736   TATGGCCATTCCGAGTTTGAACTGGCAATCGCCTTGATGTTTGGGGGGTTC
239    Y  G  H  S  E  F  E  L  A  I  A  L  M  F  G  G  F
787   CCCAGATCCTTCTTCACCGCCTACCACCGGAAGATCCCCAAGGCTCCGGGC
256    P  R  S  F  F  T  A  Y  H  R  K  I  P  K  A  P  G
838   TTCGACCAGCGGCTGCTGCTCTACCAGCTGTTTAACTACCTGAACCACTGG
273    F  D  Q  R  L  L  L  Y  Q  L  F  N  Y  L  N  H  W
889   AACCACTTCGGGCGGGAGTACAGGAGCCCTTCCTTGGGCACCATGCGAAGG
290    N  H  F  G  R  E  Y  R  S  P  S  L  G  T  M  R  R
940   CTGCTCAAGTAG
307    L  L  K
952   CCGGCCCCTGCCCTCCCTTCCCCTGTCCCCGTCCCCGTCTCTCTCCCCATC
1003  CCAAGTCATCCAGCCCTTCTCCCTGCACTCATGAAACCCCAATAAATATCC
1054  TCATTGACAACCAG
```

FIG. 8. DNA sequence and the predicted amino acid sequence of FN3K deduced from BLAST analysis and alignment of 11 human ESTs overlapping with the sequenced tryptic fragments. The underlined peptides indicate tryptic fragments identified by μLC/MS/MS of purified FN3K.

Our deduced FN3K sequence is identical with the cloned human FN3K sequence (20) in 307 of 309 residues.

To confirm that the predicted DNA sequence does indeed correspond to an expressed gene, we performed PCR amplification of high-quality cDNA from human kidney using three nested primer sets (forward primers at positions 103, 213, and 480 of the ORF and a reverse primer at position 867). Results of these studies clearly demonstrated that the deduced ORF is represented as cDNA in this library. BLAST alignment of the ORF with the Human Genome sequences database indicates that the genomic sequences for FN3K are located on chromosomes 1 and 17 of the human genome, where they are organized in six exons spanning 20 and 32 kb, respectively. It is not clear at this time which of these two genomic sequences represents the transcribed gene or whether they are both expressed as distinct isozymes.

Assessment of tissue expression of the FN3K by PCR. To ascertain the level of expression of the FN3K gene in tissues, we performed a quantitative PCR using a short conserved 3′ amplimer (680–889 bp of the ORF) on cDNAs derived from a variety of human tissues. The result of this screen (Fig. 9) is in agreement with our previous data; it suggests that FN3K appears to be present in all tissues, with the highest level of expression in the kidney.

DISCUSSION

Properties of purified FN3K. Our data indicate that the protein we purified is identical to the FN3K that was purified and cloned by Delpierre et al. (20). The only potentially important differences between the two sets of data are the discrepant K_m values; the values reported by Delpierre were significantly lower than the values we measured (Table 2). Although we have no definitive explanation for these differences, they could possibly result from the use of different pools of erythrocytes. Whereas Delpierre et al. (20) used cells from hemochromatosis patients, we used outdated red blood cells from a blood

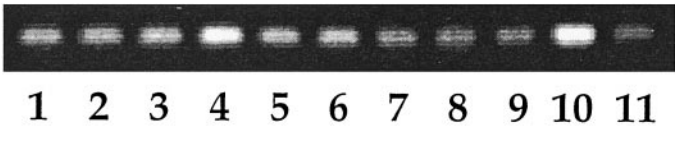

FIG. 9. PCR of cDNAs from 11 human tissues using an amplimer for the 680- to 889-bp region of the ORF. *Lane 1*, spleen; *lane 2*, lymph node; *lane 3*, thymus; *lane 4*, heart; *lane 5*, brain; *lane 6*, pancreas; *lane 7*, lung; *lane 8*, liver; *lane 9*, skeletal muscle; *lane 10*, kidney; *lane 11*, placenta.

TABLE 2
K_m values for purified FN3K

Substrate	This study	Delpierre et al. (20)
Morpholinofructose	500	1.0
FL	750	13.2
Fructoseglycine	6,500	~1000

Data are expressed as micromoles per liter.

bank. Because cells from hemochromatosis patients are younger on average than cells from unaffected individuals, and because these cells are not stored for as long as outdated blood-bank cells (>6 weeks), the observed K_m differences may reflect real differences in properties of FN3K attributable to the aging of this protein. This issue is of obvious interest and is presently under investigation.

We believe that, notwithstanding the differences in absolute K_m values between our findings and those of Delpierre et al. (20), our data on the relative affinities of various substrates (Fig. 1) are robust. It is also indicative of the fact that highly basic glycated proteins, such as histones and cytochrome C, are the preferred substrates of FN3K. Such selective affinity makes sense because these lysine-rich proteins are likely to be the ones most heavily glycated.

Physiological significance. The coexistence of high concentrations of glucose and lysine at 37°C inevitably leads to Maillard reactions. Abundant experimental data suggest that products of these reactions (both the early and advanced products) are harmful to cell function (30–33). Because of this demonstrable toxicity, it may be expected that homeothermic animals will have developed mechanisms to minimize this damage. Kinetic analysis of the early stages of the Maillard reaction suggests that an effective intervention would be the decomposition of the Amadori intermediate (FL) (Fig. 10). Based on this consideration, several laboratories have made efforts to identify enzymes that could cleave the fructosamine linkage (Amadoriases). As a results of these investigations, a number of microbial Amadoriases have been characterized (34–38). These enzymes catalyze the decomposition of Amadori compounds by one of two oxidative routes: *1*) oxidation of the aminoketose to fructosamine (1-amino-1-deoxy-fructose) and a deaminated base (34), or *2*) oxidation of fructosamine to glucosone and an unmodified amine (35–37). Significantly, these microbial enzymes cannot however use protein-bound Amadori products as substrates (34,35,38), and their counterparts have not been found in mammalian organisms.

The discovery of FN3K is the first indication of a potential system for controlling the Maillard reaction in higher organisms. In addition to human erythrocytes, in which this enzyme is quite active, we have obtained evidence of FN3K expression and/or activity in every cell and tissue examined thus far. Because of its ubiquitous distribution, we postulate that FN3K may be important for the function and survival of some cells. Its involvement in the control of intracellular nonenzymatic glycation may entail one or both of the following mechanisms: *1*) phosphorylation of the fructosamine adducts on proteins may serve as a marker for degradation of glycated proteins by a specific proteolytic process, and/or *2*) formation of FL3P may be a means of removing Amadori adducts from glycated proteins (Fig. 11).

Based on the intrinsic lability of FL3P, we tend to favor the second hypothesis. Furthermore, recent studies on FL metabolism in rats indicate that rat kidneys that have high levels of FN3K activity also appear to possess an enzyme (or enzymes) that may catalyze the decomposition of FL3P to 3DG (39). Such deglycation could be particularly important for long-lived basic intracellular proteins, such as histones, some of which turn over very slowly, even in rapidly growing cells (40).

Although the postulated function of FN3K as a deglycating enzyme has not yet been tested directly, this hypothesis is supported indirectly by studies on the sites of nonenzymatic glycation of Hb. When unmodified Hb is incubated with glucose in vitro, the glycation of lysine residues significantly exceeds that of β-terminal valine, and the pattern of glycosylation of particular lysines differs from that observed in vivo (41–43). In contrast, the analysis of glycation sites in HbA_{1c} obtained from normoglycemic individuals and diabetic patients reveals that the dominant glycation site in vivo is the terminal valine of the β-chain, while there is significantly less modification of the more numerous lysine residues (41–43). In the context of the proposed deglycation scheme, this discrepancy can be explained by the fact that fructosevaline is a much poorer substrate for FN3K than FL (Fig. 1). Consequently, one would predict that in vivo, FL would be broken down far more efficiently than fructosevaline, resulting in a greater accumulation of the latter compound.

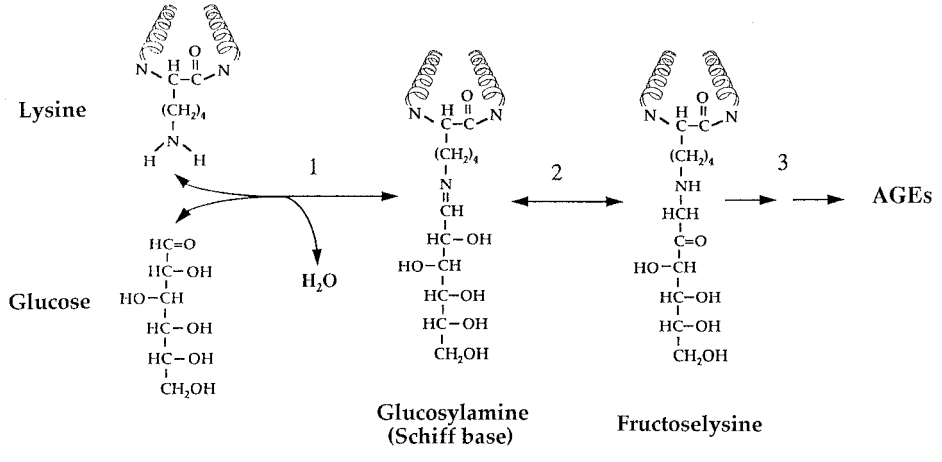

FIG. 10. Outline of the initial steps of the Maillard reaction between lysine and glucose. Both first stages of this reaction are reversible, but step 1 (formation of glucosylamine [Schiff base]) is much faster than step 2 (formation of fructosamine).

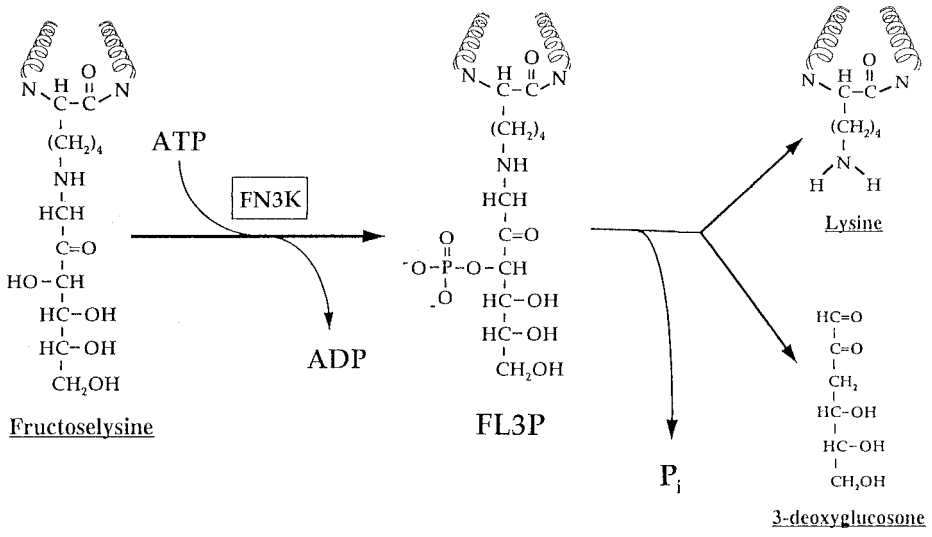

FIG. 11. Proposed role of FN3K as a catalyst in the decomposition of FL. Phosphorylation of FL to FL3P destabilizes the fructoselysine linkage and leads to a spontaneous decomposition of FL to lysine, inorganic phosphate (P_i), and 3DG. Preliminary data suggest that this decomposition step may be catalyzed in vivo by a specific hydrolase (39).

One potential difficulty with the proposed deglycation mechanism is the fact that, in the process of breaking down FL residues, FN3K produces a reactive by-product (3-DG). As documented in several studies, this ketoaldehyde is a potent glycating agent that can inactivate enzymes, inhibit cell growth and replication (44,45), and may be involved in diabetic embryopathy (46). Thus, for the FN3K-deglycation system to operate properly, along with FN3K, cells must have systems to detoxify 3DG. Such enzymes, which catalyze the reduction of 3DG to 3-deoxyfructose (3DF) (47–50) and its oxidation to 3-deoxy-2-ketogluconic acid (DGA) (51,52), have been identified in a number of tissues and appear to be widely distributed. Therefore, we postulate that, under normoglycemic conditions, the FN3K system functions efficiently by keeping the levels of glycated proteins in check by breaking down FL residues to lysine, 3DG, and inorganic phosphate and by metabolizing the resultant 3DG to 3DF and DGA. Such a two-stage detoxification system is not uncommon in nature, as illustrated by the superoxide-dismutase/catalase system. Superoxide dismutase detoxifies superoxide radicals by converting them to a less reactive but still toxic hydrogen peroxide (53). This primary detoxification product is then converted by catalase to the final products of water and oxygen (54). Absence or deficiency of either of these protective enzymes results in major detrimental effects on cell function (54,55).

An interesting and totally unexpected finding of our study is the nonlinear relationship between FL3P and HbA_{1c}, and the virtual absence of FL3P at low or modest hyperglycemia at HbA_{1c} of <8%. This relationship between FL3P-Hb and HbA_{1c} is reminiscent of the apparent nonlinear relationship between HbA_{1c} and the incidence of long-term diabetic complications in the Diabetes Control and Complications Trial (DCCT) population (56) and is consistent with recent reports of an apparent glycemic threshold for the formation of AGEs and cataracts in the diabetic lens (57,58). Several possible mechanisms could be postulated to account for this nonlinear relationship. Probably the most intriguing possibility is that red blood cells may possess another deglycating system that prevents the accumulation of FL3P and FL by controlling the rate of formation of the Schiff base (Fig. 10). There are some preliminary data suggesting that levels of Schiff bases in red blood cells are controlled (59); however, definitive evidence for such a system has yet to be obtained.

In conclusion, the discovery of FN3K in human tissues suggests a new paradigm for thinking about the process of nonenzymatic glycation. If the postulated deglycating function of FN3K is confirmed by future investigations, this finding should be helpful in producing a better understanding of nonenzymatic glycation and its relationship to long-term diabetic complications.

ACKNOWLEDGMENTS

The research described herein was supported by National Institutes of Health Grants DK-57146, DK-50364, EY-08414, an American Diabetes Association Research Grant to B.S.S., a Juvenile Diabetes Foundation grant to P.J.B., and the New Hampshire chapter of the Fraternal Order of the Eagles.

This study is dedicated to the memory of Dr. Martin Weingarten.

REFERENCES

1. Monnier VM: The Maillard reaction in aging: diabetes and nutrition. *Prog Clin Biol Res* 304:1–22, 1989
2. Lendl F, Schleicher E: New aspects of the Maillard reaction in foods and in the human body. *Angewandte Chemie* 29:565–706, 1990
3. Mossine VV, Glinsky GV, Feather MS: The preparation and characterization of some Amadori compounds (1-amino-1-deoxy-D-fructose derivatives) derived from a series of aliphatic w-amino acids. *Carbohydr Res* 262:257–270, 1994
4. Roper H, Roper S, Heyns K: NMR spectroscopy of N-(1-deoxy-D-fructos-1-yl)-L-amino acids ("fructose-amino acids"). *Carbohydr Res* 116:183–195, 1983
5. Carson JF: The reaction of fructose with isopropylamine and cyclohexylamine. *J Am Chem Soc* 77:1881–1884, 1955
6. Heyns K, Eichstedt R, Meinecke KH: Die umsetzung von fructose und sorbose mit ammoniak und aminen. *Chem Berichte* 88:1551–1555, 1955
7. Sell DR, Monnier VM: Structure elucidation of a senescence cross-link from human extracellular matrix: implication of pentoses in the aging process. *J Biol Chem* 264:21597–21602, 1989
8. Nagaraj RH, Shipanova IN, Faust FM: Protein cross-linking by the Maillard reaction: isolation, characterization, and in vivo detection of a lysine-lysine cross-link derived from methylglyoxal. *J Biol Chem* 271:19338–19345, 1996
9. Requena JR, Ahmed MU, Fountain CW, Degenhardt TP, Reddy S, Perez C, Lyons TJ, Jenkins AJ, Baynes JW, Thorpe SR: Carboxymethyl-ethanol-

amine: a biomarker of phospholipid modification during the Maillard reaction in vivo. *J Biol Chem* 272:17473–17479, 1997
10. Reddy S, Bichler J, Wells-Knecht KJ, Thorpe SR, Baynes JW: N epsilon-(carboxymethyl)lysine is a dominant advanced glycation end product (AGE) antigen in tissue proteins. *Biochemistry* 34:10872–10878, 1995
11. Bucala R, Cerami A: Advanced glycosylation: chemistry, biology, and implications for diabetes and aging. *Adv Pharmacol* 23:1–34, 1992
12. Lyons TJ, Jenkins AJ: Glycation, oxidation and lipoxidation in the development of the complications of diabetes: a carbonyl stress hypothesis. *Diabetes Rev* 5:365–391, 1997
13. Beisswenger PJ, Makita Z, Curphey TJ, Moore LL, Jean S, Brinck-Johnsen T, Bucala R, Vlassara H: Formation of immunochemical advanced glycosylation end products precedes and correlates with early manifestations of renal and retinal disease in diabetes. *Diabetes* 44:824–829, 1995
14. King GL, Brownlee M: The cellular and molecular mechanisms of diabetic complications. *Endocrin Metab Clinics North America* 25:255–270, 1996
15. Szwergold BS, Kappler F, Brown TR: Identification of fructose-3-phosphate in the lens of diabetic rats. *Science* 247:451–454, 1990
16. Lal S, Szwergold BS, Taylor AH, Randall WC, Kappler F, Wells-Knecht K, Baynes JW, Brown TR: Metabolism of fructose-3-phosphate in the diabetic rat lens. *Arch Biochem Biophys* 318:191–199, 1995
17. Szwergold BS, Taylor K, Lal S, Su B, Kappler F, Brown TR: Identification of a novel protein kinase activity specific for Amadori adducts on glycated proteins (Abstract). *Diabetes* 46 (Suppl. 1):108A, 1997
18. Lal S, Szwergold BS, Kappler F, Brown TR: Detection of fructose-3-phosphokinase: activity in intact mammalian lenses by 31P NMR spectroscopy. *J Biol Chem* 268:7763–7767, 1993
19. Petersen A, Kappler F, Szwergold BS, Brown TR: Fructose metabolism in the human erythrocyte: phosphorylation to fructose-3-phosphate. *Biochem J* 284:363–366, 1992
20. Delpierre G, Rider MH, Collard F, Stroobant V, Santos H, Van Schaftingen E: Identification, cloning, and heterologous expression of a mammalian fructosamine-3-kinase. *Diabetes* 49:1627–1634, 2000
21. Finot PA, Mauron J: Le blocage de la lysine par la reaction de Maillard. I. Synthese de N-(desoxy-1-D-fructosyl-1)-et N-(desoxy-1-D-lactulosyl-1)-L-lysines. *J Helv Chim Acta* 52:1488–1495, 1969
22. Lal S, Kappler F, Walker M, Orchard TJ, Beisswenger PJ, Szwergold BS, Brown TR: Quantitation of 3-deoxyglucosone levels in human plasma. *Arch Biochem Biophys* 342:254–260, 1997
23. Beutler E: A manual of biochemical methods. In *Red Cell Metabolism*. New York, Grune & Stratton, 1971, p. 13–14
24. Delahunty T: Convenient screening for hemoglobin variants by using the Diamat HPLC system. *Clin Chem* 36:903–905, 1990
25. Robitaille PM, Robitaille PA, Brown GG, Brown GG: Analysis of the pH-dependent chemical shift behavior of phosphorus-containing metabolites. *J Magn Reson* 92:73–84, 1991
26. Baynes JW, Thorpe SR, Murtiashaw MH: Nonenzymatic glucosylation of lysine residues in albumin. *Methods Enzymol* 106:88–98, 1984
27. Gorenstein DG: Phosphorus-31: nuclear magnetic resonance of enzyme complexes: bound ligand structure, dynamics, and environment. *Methods Enzymol* 177:295–316, 1989
28. Bunn HK, Gabbay K, Gallop P: The glycosylation of hemoglobin: relevance to diabetes mellitus. *Science* 200:21–27, 1978
29. Nathan DM, Singer DE, Hurxthal K, Goodson JD: The clinical information value of the glycosylated hemoglobin assay. *N Engl J Med* 310:341–346, 1984
30. Hirata C, Nakano K, Nakamura N, Kitagawa Y, Shigeta H, Hasegawa G, Ogata M, Ikeda T, Sawa H, Nakamura K, Ienaga K, Obayashi H, Kondo M: Advanced glycation end products induce expression of vascular endothelial growth factor by retinal Muller cells. *Biochem Biophys Res Comm* 236:712–715, 1997
31. McVerry BA, Fisher C, Hopp A, Huens ER: Production of pseudodiabetic renal glomerular changes in mice after repeated injections of glucosylated proteins. *Lancet* 738–740, 1980
32. Sabbatini M, Sansone G, Uccello F, Golberti A, Conte G, Andreucci VE: Early glycosylation products induce glomerular hyperfiltration in normal rats. *Kidney Inter* 42:875–881, 1992
33. Ziyadeh FN, Cohen MP: Effects of glycated albumin on mesangial cells: evidence for a role in diabetic nephropathy. *Mol Cell Biochem* 125:19–25, 1993
34. Saxena AK, Saxena P, Monnier VM: Purification and characterization of a membrane-bound deglycating enzyme (1-deoxyfructosyl alkyl amino acid oxidase, EC 1.5.3) from a *Pseudomonas* sp. soil strain. *J Biol Chem* 271:32803–32809, 1996
35. Takahashi M, Pischetsrieder M, Monnier VM: Isolation, purification, and characterization of amadoriase isoenzymes (fructosyl amine-oxygen oxioreductase EC 1.5.3) from *Aspergillus* sp. *J Biol Chem* 272:3437–3443, 1997
36. Takahashi M, Pischetsrieder M, Monnier VM: Molecular cloning and expression of amadoriase isoenzyme (fructosyl amine:oxygen oxidoreductase, EC 1.5.3) from *Aspergillus fumigatus*. *J Biol Chem* 272:12505–12507, 1997
37. Horiuchi T, Kurokawa T, Saito N: Purification and properties of fructosyl-amino acid oxidase from *Corynebacterium* sp. 2-4-1. *Agr Biol Chem*. 53:103–110, 1989
38. Yoshida N, Sakai Y, Isogai A, Fukuya H, Yagi M, Tani Y, Kato N: Primary structures of fungal fructosyl amino acid oxidases and their application to the measurement of glycated proteins. *Eur J Biochem* 242:499–505, 1996
39. Kappler F, Djafroudi S, Kayser H, Su B, Lal S, Randall WC, Walker MA, Taylor A, Szwergold BS, Erbersdobler H, Brown TR: Metabolism of fructoselysine in the kidney. In *Proceedings of the Sixth International Maillard Symposium*, London, 1997. O'Brian J., Nursen H.E., Crabbe M.J.C., Ames J.M., Eds. Cambridge, U.K., The Royal Society of Chemistry, p. 415
40. Tsvetkov S, Ivanova E, Djondjurov L: Metabolic behaviors of the core histones in proliferating Friend cells. *Exp Cell Res* 180:94–105, 1989
41. Bunn HF, Shapiro R, McManus MJ, Garrick L, McDonald, Gallop P, Gabbay KH: Structural heterogeneity of human hemoglobin A due to nonenzymatic glycosylation. *J Biol Chem* 254:3892–3898, 1979
42. Shapiro R, McManus MJ, Zalut C, Bunn HF: Sites of nonenzymatic glycosylation of human hemoglobin A. *J Biol Chem* 255:3120–3127, 1980
43. Garlick RL, Mazer JS, Higgins PJ, Bunn HF: Characterization of glycosylated hemoglobins: relevance to monitoring of diabetic control and analysis of other proteins. *J Clin Invest* 71:1062–1072, 1983
44. Shinoda T, Hayase F, Kato H: Suppression of cell-cycle: progression during the s-phase of rat fibroblasts by 3-deoxyglucosone, a Maillard reaction intermediate. *Biosci Biotech Biochem* 58:2215–2219, 1994
45. Okado A, Kawasaki Y, Hasuike Y, Takahashi M, Teshima T, Fujii J, Taniguchi N: Induction of apoptotic cell death by methylglyoxal and 3-deoxyglucosone in macrophage-derived cell lines. *Biochem Biophys Res Comm* 225:219–224, 1996
46. Eriksson UJ, Wentzel P, Minhas HS, Thornalley PJ: Teratogenicity of 3-deoxyglucosone and diabetic embryopathy. *Diabetes* 47:1960–1966, 1998
47. Kato H, van Chuyen N, Shinoda T, Sekiya F, Hayase F: Metabolism of 3-deoxyglucosone, an intermediate compound in the Maillard reaction, administered orally or intravenously to rats. *Biochim Biophys Acta*, 1035:71–76, 1990
48. Takahashi M, Fujii J, Teshima T, Suzuki K, Shiba T, Taniguchi N: Identity of a major 3-deoxyglucosone-reducing enzyme with aldehyde reductase in rat liver established by amino acid sequencing and cDNA expression. *Gene* 127:247–253, 1993
49. Liang ZQ, Hayase F, Kato H: Purification and characterization of NADPH-dependent 2-oxoaldehyde reductase from porcine liver: a self-defense enzyme preventing the advanced stage of the Maillard reaction. *Eur J Biochem* 197:373–379, 1991
50. Sato K, Inazu A, Yamaguchi S, Nakayama T, Deyashiki Y, Sawada H, Hara A: Monkey 3-deoxyglucosone reductase: tissue distribution and purification of three multiple forms of the kidney enzyme that are identical with dihydrodiol dehydrogenase, aldehyde reductase, and aldose reductase. *Arch Biochem Biophys* 307:286–294, 1993
51. Oimoni M, Hata F, Igaki N, Nakamichi T, Baba S, Kato S: Purification of α-ketoaldehyde dehydrogenase from the human liver and its possible significance in the control of glycation. *Experientia* 45:463–466, 1989
52. Fujii E, Iwase H, Ishii-Karakasa I, Yajima Y, Hotta K: The presence of 2-keto-3 deoxygluconic acid and oxoaldehyde dehydrogenase activity in human erythrocytes. *Biochem Biophys Res Comm* 210:852–857, 1995
53. Peskin AV: Cu,Zn-superoxide dismutase gene dosage and cell resistance to oxidative stress: a review. *Biosci Rep* 17:85–89, 1997
54. Willekens H, Chamnongpol S, Davey M, Schraudner M, Langebatels C, Van Montagu M Inze D, Van Camp W: Catalase is a sink for H2O2 and is indispensable for stress defense in C3 plants. *EMBO J* 16:4806–4816, 1997
55. Auclair C, Dhermy D, Boivin P: Intravascular hemolysis in patients with superoxide dismutase deficiency: further evidence for the protective role of superoxide dismutase in aerobic cells. *Bull Europ Physiopathol Respert* 17 (Suppl.):207–211, 1991
56. Krolewski AS, Warram JH, Freire MB: Epidemiology of late diabetic complications: a basis for the development and evaluation of preventive programs. *Endocrin Metab Clin North Ame* 25:217–242, 1996
57. Nagaraj RH, Kern TS, Sell DR, Fogarty J, Engerman RL, Monnier VM: Evidence of a glycemic threshold for the formation of pentosidine in diabetic dog lens but not in collagen. *Diabetes* 45:587–594, 1996
58. Swami-Mruthinti, Shaw SM, Zhao HR, Green K, Abraham EC: Evidence of a glycemic threshold for the development of cataracts in diabetic rats. *Curr Eye Res* 18:423–429, 1999
59. Mortensen HB, Marshall MO: Effects of saline incubation on red cell content of glucosylated hemoglobins studied by iso-electric focusing. *Clin Chim Acta* 132:213–217, 1983